Zitierweise:
doi.org/10.1002/anie.202303103

DNA Nanotechnology

Functional Nanopores Enabled with DNA

Yongzheng Xing[+],* *Alexia Rottensteiner*[+], *Jonah Ciccone, and Stefan Howorka**

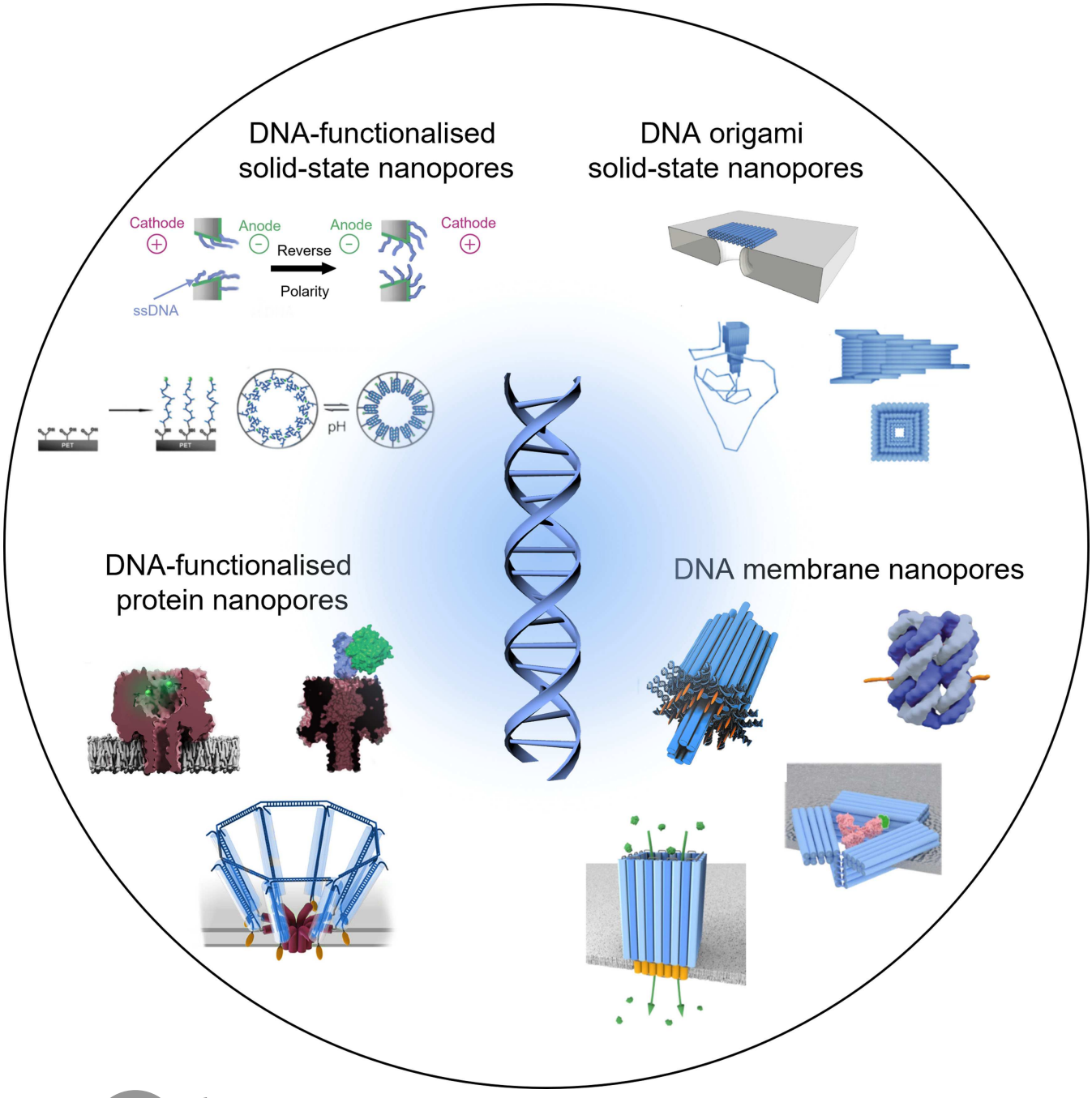

Abstract: Membrane-spanning nanopores are used in label-free single-molecule sensing and next-generation portable nucleic acid sequencing, and as powerful research tools in biology, biophysics, and synthetic biology. Naturally occurring protein and peptide pores, as well as synthetic inorganic nanopores, are used in these applications, with their limitations. The structural and functional repertoire of nanopores can be considerably expanded by functionalising existing pores with DNA strands and by creating an entirely new class of nanopores with DNA nanotechnology. This review outlines progress in this area of functional DNA nanopores and outlines developments to open up new applications.

1. Introduction

Nanopores are nanoscale holes within a thin membrane and allow transport of molecular cargo from either side of the membrane. In biology, protein nanopores embedded in lipid bilayers fulfil essential roles in ion flux,[1] cellular signalling[2] and immunobiological defence.[3] Outside biology, nanopores can be used for label-free sensing. Conventionally, nanopore sensing is performed using two electrolyte-filled chambers separated by an insulating membrane with an embedded nanopore (Figure 1a). The passage of analyte molecules through the nanopore temporarily blocks the flow of ions which causes a characteristic signal in the measured current (Figure 1b).[4–12] The magnitude and frequency of ionic current blockades reveal information on the size and concentration of the analyte at single-molecule level.[13,14] Analytes can include proteins,[9,15,16] peptides,[17–19] RNA[20] and DNA.[21–23] Importantly, nanopores have enable label-free, portable, and long-read DNA sequencing.[24–26] Beyond sensing and sequencing, nanopores have been used as research tools in cell biology, or in biomimetic research and synthetic biology.[4] For these applications, nanopores should ideally have defined sizes, specific molecular interaction properties, or be able to change in shape, depending on the specific use. To meet these criteria, protein pores have been engineered, while new pores with tailored properties have been developed with inorganic materials as well as DNA.

1.1. Protein and peptide pores

Protein pores are biologically occurring membrane channels formed of proteins. They are the most commonly used nanopores for sensing applications. One such protein pore is the pore-forming toxin α-haemolysin (αHL) (Figure 1c).[27] αHL is a heptameric membrane channel protein from *Staphylococcus aureus* which forms water-filled channels on the plasma membrane of erythrocytes and other eukaryotic cells resulting in the loss of cell-relevant molecules and ultimately cell lysis or death. With an internal lumen diameter that varies between 2.9 nm at the *cis* entrance, 4.1 nm in the internal cavity, 1.3 nm at the inner constriction, and 2 nm at the *trans* entrance of the β-barrel,[27] αHL was the first nanopore to record ionic current changes upon translocation of DNA and RNA polymers[13,28] and has been used for many other sensing applications. Other protein pores used for sensing include *Mycobacterium smegmatis* porin A (MspA)[29] and bacterial outer membrane channel CsgG[26,30] with the latter being utilised in commercial equipments from Oxford Nanopore Technologies for nanopore-based DNA and RNA sequencing. Sensing has also been explored with the PA_{63} channel of anthrax toxin,[31] the potassium channel KscA,[32] the toxin aerolysin,[7,33] the mechanosensitive channel MscL,[34] the bacterial transporter FhuA,[9,35] the bacterial toxin ClyA,[36] and the bacteriophage phi29 DNA packaging motor.[37] Biological nanopores are advantageous for commercial products as biological protein expression enables the large-scale fabrication of nanopores with precise and consistent geometry. Consistent geometry is essential when nanopores are used as single-molecule sensors where read-out intimately depends on the structure of the nanopore.

Adapting nanopores for many sensing applications requires structural features that are less abundant in naturally occurring protein nanopores. Protein nanopores have been extensively mutated[38] to acquire specific properties desirable for sensing, such as size-selectivity or specific molecular interaction. For example, an MspA-based nanopore sensing platform was reported[39] in which a rationally designed polymer strand was tethered to the MspA pore. This enabled single-molecule detection of a wide range of analytes, monitoring of chemical reactions, and discrimination of enantiomers.[40] Modifications of protein pores can be introduced by replacing,[41] deleting,[42,43] or adding amino acids[44] and thereby changing the surface charges,[45] functional groups[46] and hydrophobicity[47] of the pore, as shown by Soskine et al. for the ClyA pore.[48] These specific mutations can alter the pores' stability in response to changes in pH[49] or salt concentration.[50] Nevertheless, the introduction of several chemical modifications makes the fabrication of pores of predictable structure difficult.

Peptide pores of small dimensions allow higher design versatility by simple inclusion of amino acid residues outside of the conventional remit of L-amino acids.[51,52] Peptides also facilitate the complete de novo design of highly tuneable designer pores from non-proteinogenic amino acids.[53,54] Inspired by the structure of naturally occurring antibiotic gramicidin pores, synthetic peptide pores have

[*] Dr. Y. Xing,[+] Dr. A. Rottensteiner,[+] Dr. J. Ciccone, Prof. S. Howorka
Department of Chemistry, Institute for Structural and Molecular Biology, University College London
London WC1H 0AJ (UK)
E-mail: y.xing@ucl.ac.uk
s.howorka@ucl.ac.uk

[+] These authors contributed equally to this work.

been designed to act as antibiotic agents by rupturing the bacterial membranes.[53,55] Furthermore, peptide pores have been used for label-free sensing.[56] Advantages of peptide pores include their facile fabrication via solid phase synthesis, their ability to easily insert into membranes due to their small dimensions, and the high freedom in structural design. Nevertheless, de novo design of synthetic peptide pores allows only the construction of small pores[57,58] but this is currently changing with breakthroughs in predicting the structure of proteins.

Despite the ability to introduce minor modifications, large-scale re-design of a protein or peptide pore is often difficult. One such example of challenging modifications is to enlarge the aperture of the nanopore. As most biological pores have lumen sizes under 2 nm, expanding this to 5 nm and beyond would significantly expand the array of potential analytes. While very large-aperture protein nanopores do exist,[59,60] they suffer from issues in low stability and low homogeneity in oligomerisation.[61,62]

1.2. Solid-state nanopores

Solid-state nanopores (Figure 1d) address several of the shortcomings of protein pores and are commonly fabricated from inorganic thin membrane sheets by etching a hole,[63,64] via electron[65] or ion-beam drilling,[66] or by using glass nanopipettes.[67,68] To avoid the need of the costly drilling approches, nanopores can also be made via dielectric breakdown.[69,70] The non-biological nature of solid-state nanopores renders them stable to a far wider array of conditions than protein nanopores. Solid-state pores can also be generated with highly customisable lumen sizes and adjustable surface properties.[64,65,71,72] Because of these advantages, solid-state nanopores are currently leading the field of large-aperture nanopore sensing.[73,74]

Analyte detection using solid-state nanopores faces challenges due to high analyte translocation velocity, inconsistent pore geometry, and lower resolution on pore chemistry than atomistic-defined protein pores. The passage of small analytes through the large lumen of a solid-state nanopore can occur too rapidly to yield measurable signals. To overcome this issue, molecular modifications[75] and nanobeads[76] have been incorporated in the pores to slow translocation. A further limitation of solid-state nanopores is associated with the wide lumen and inconsistent lumen geometry which hinders the generation of reproducible signals. While 1 nm-narrow can be achieved with carbon nanotubes[77] or atomically thin 2D materials such as MoS_2[78,79] there is also considerable scope in modifying the lumen of wider solid-state nanopores in thicker membrane materials, such as the tethering of oligonucleotides to the pore walls or the insertion of DNA nanostructures into the lumen.

1.3. DNA modification and DNA nanotechnology

DNA offers a route to address several of the shortcomings of existing protein, peptide and solid-state pores either by adding single or double-stranded DNA or by building entirely DNA-based nanopores. The well-understood base-

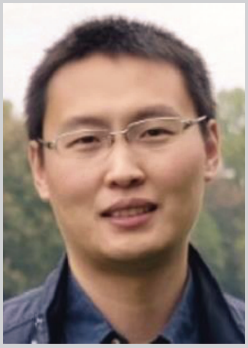

Yongzheng Xing completed his Ph.D. with Prof. Dongsheng Liu at Tsinghua University and National Center for Nanoscience and Technology. He conducted his postdoctoral research with Prof. Tim Liedl (LMU Munich) and Prof. Stefan Howorka (UCL). His current research interests include the creation of novel DNA nanostructures and their functionalization for nanopore sensing, biomimetic nanodevices and smart materials.

Alexia Rottensteiner completed a Master's in Chemical Research at UCL and subsequently joined the group of Prof. Howorka at UCL as Ph.D. student. Her Ph.D. studies focus on the fabrication of membrane-interacting DNA nanostructures and the investigation of DNA channels. Alexia is currently completing her Ph.D. and working as a researcher in Howorka's group. Her research interests include functional DNA origami devices, DNA nanostructure membrane interaction and DNA pores.

Jonah Ciccone completed his Master with Dr. McDowall at University of Leeds in 2015 studying leaderless translation. He then went on to work as a DNA Scientist with Oxford Nanopore Technologies before joining the Howorka research group in 2019 to complete a Ph.D. focussing on strategies to insert synthetic DNA nanopores into polymeric membranes for bio-sensing applications.

Stefan Howorka is a Professor of Chemical Biology at the Department of Chemistry at UCL. He obtained his Ph.D. from the University of Vienna in 1999 and performed his postdoctoral studies at Texas A&M University. After 3 years at a biotech incubator, he joined UCL and was promoted to Professor in 2016. His research interests include the characterization of biological protein and peptide pores, the design of synthetic membrane nanopores for biosensing, and the development of research tools for membrane biophysics. He has licensed a protein pore technology for widely used portable, DNA sequencing.

pairing properties of DNA are the basis for DNA nanotechnology[80–83] which provides unprecedented flexibility to design and build customised nanostructures of well-defined dimensions[80,84–87] and functions.[88,89] Coupled with well-established DNA modification methodologies, DNA nanostructures are used as a structural scaffold to organise nano-objects,[90–94] assemble and control chemical or enzymatical reactions,[95–97] and guide the assembly of biological and chemical molecules.[98,99]

In this review, we will focus on recent progress in building functional nanopores enabled with DNA modification and DNA nanotechnology. We first cover how DNA modification of established protein pores can expand their function, and how DNA nanostructures can act as structural templates to guide the precise assembly of pore-forming peptides and proteins. The review will then describe how solid-state nanopores are modified with DNA oligonucleotides and DNA nanostructures to redefine the geometry or functionality of the pore. We will finally summarise the de novo fabrication of DNA nanopores that puncture biological and synthetic membranes (Figure 1e). DNA nanopores have been reviewed previously.[100] Readers interested in DNA-related analytical applications are guided to reviews by Ying et al.,[101] Liu et al.,[102] and Ding et al.[103]

2. DNA-functionalised protein and peptide nanopores

Protein nanopores have been functionalised with DNA oligonucleotides to impart desirable properties, such as increasing the residence time of translocating analytes. Electrophoretically propelled DNA analytes can translocate through the barrel of a short nanopore faster than the scan rate of the electrical amplifier leading to poorly resolved current signals. As one route to reduce the translocation speed, Howorka et al. allowed the oligonucleotide to hybridise to a complementary oligonucleotide sequence conjugated into the lumen of an αHL pore (Figure 2a).[105] Variation in the residence time of the oligonucleotides spent inside αHL enabled precise discrimination of single base mutations within the translocating oligonucleotide. This setup also helped explore the kinetics of DNA strand hybridisation (Figure 2b),[106] as well as probing the internal geometry of αHL.[107] The work on DNA duplex sensing was preceded by the analysis of transient duplexes formed by hairpin structures inside the pore.[108] The studies on DNA-modified protein pores were expanded by Rotem et al. In their study, a DNA aptamer was used to enable specific protein recognition (Figure 2c).[8] Given the large size of the analyte, the aptamer was positioned at the pore entrance to allow the binding of the protein outside the pore. Later, Soskine et al. reported the conjugation of DNA aptamers on a larger pore, ClyA, and realised the selective capturing of proteins into the pore lumen.[48] The potential of non-covalent DNA-modification was further explored by Fanceschini et al.[109]

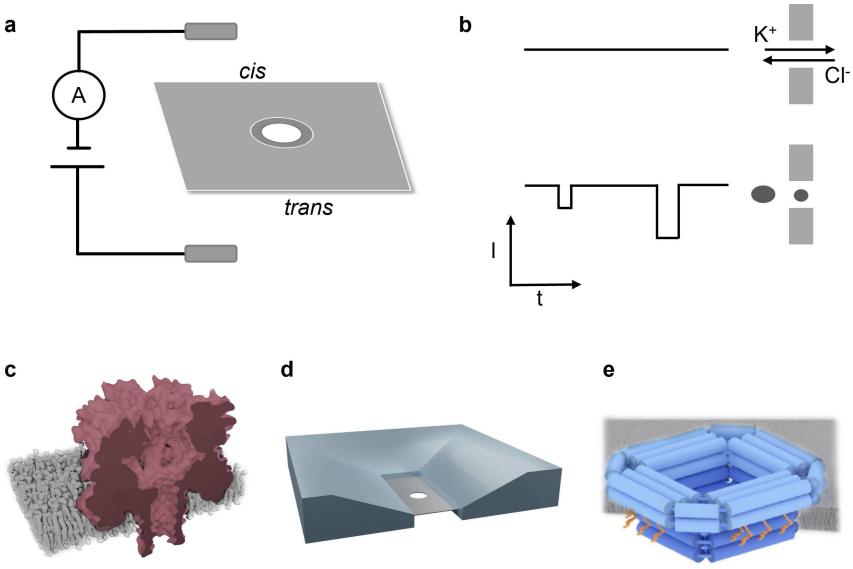

Figure 1. Schematic representations of nanopore sensing and nanopore systems. a) Simplified circuit diagram showing the setup of electrical current recordings through a nanopore placed inside a membrane (grey). b) The principle of nanopore-based label-free sensing. Top: A transmembrane potential causes a constant flow of electrolyte ions through a single pore. Bottom: The passage of analytes (dark grey spheres) temporarily impedes the ion flow resulting in characteristic changes in the recorded current displayed as current blockades in single-channel current traces plotting current, *I*, vs. time, *t*. c) Molecular model of the protein nanopore α-hemolysin (αHL) inserted in lipid bilayer membrane. d) Schematic 3D model of a solid-state nanopore. e) Schematic drawing of a DNA origami nanopore composed of DNA duplexes (blue cylinders). Membrane anchors (orange) insert the pore in a lipid bilayer. Adapted with permission from Ref. [104], Copyright 2022 Nature Publishing Group.

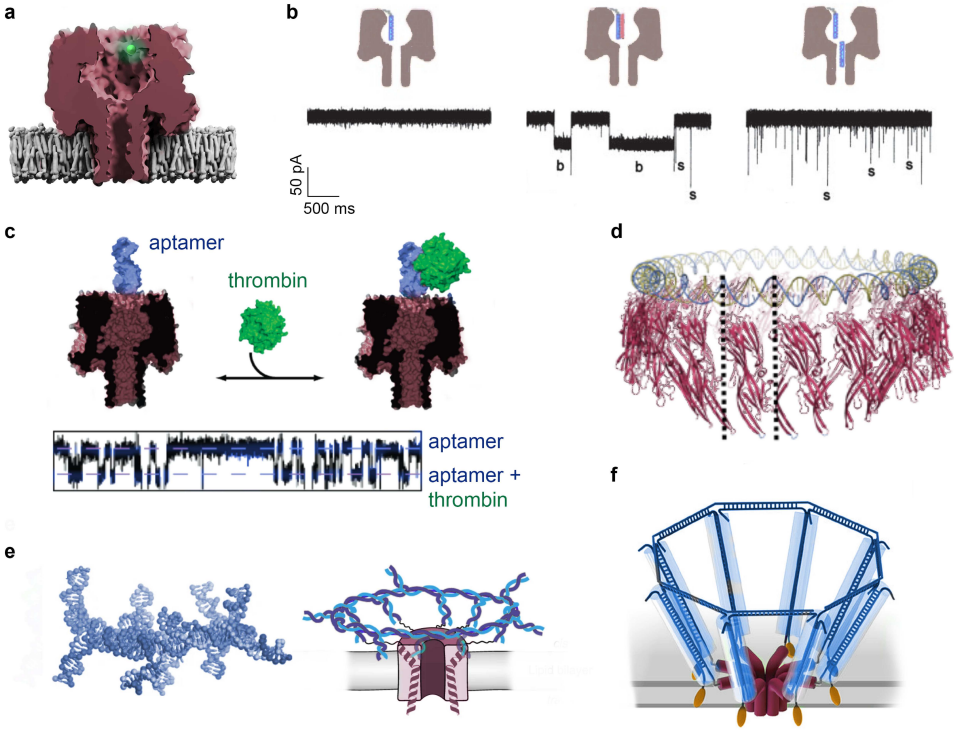

Figure 2. DNA-functionalised protein and peptide nanopores. a) An αHL pore with an engineered cysteine residue (green dot) for covalently attaching a single-stranded DNA molecule. b) An αHL pore carrying a DNA strand (blue) allows hybridization with a complementary DNA strand (red) to yield current blockades that help determine the kinetics of DNA duplex formation via single-channel current recordings (middle panel, bottom). Free unbound strands (blue) not complementary to the tethered strand translocate fast through the pore without causing long blockades (right panel, bottom). Adapted with permission from Ref. [106], Copyright 2001 National Academy of Sciences. c) A DNA aptamer (blue) attached to the aHL pore enables specific binding of a thrombin protein (green) as monitored in a single-channel current trace (bottom). Adapted with permission from Ref. [8], Copyright 2012 American Chemical Society. d) A DNA hybrid pore featuring a DNA duplex scaffold which assembles multiple αHL monomers (red). The black dashed lines indicate a single protein subunit. Adapted with permission from Ref. [112], Copyright 2017 Nucleic Acids Research. e) Coarse-grained molecular dynamics simulation of a DNA scaffold (left) and the schemetic drawing of a DNA scaffold-templated pore of attached Wza peptide (red) inserted into lipid bilayer (right). Adapted with permission from Ref. [113], Copyright 2018 Nature Publishing Group. f) DNA nanostructure-guided assembly of DNA-modified peptide CtXa (red) monomers to form a membrane-spanning pore. Adapted with permission from Ref. [114], Copyright 2021 American Chemical Society.

The study followed previous investigations where a DNA-PEG strand was threaded into the αHL pore to form a rotaxane.[110] In the case of ClyA, DNA modifications installed at one pore side helped achieve the controlled and hybridization-mediated transport of another, threaded DNA strand across the pore lumen. The functional repertoire of protein pores has also been expanded with analyte-sensing polymers,[15] adaptors that reside within the pore and accommodate nucleotides[21] or via covalent small-molecule modifications.[111]

In addition to modifying existing pores, DNA has been used to expand the structural repertoire of protein pores by acting as an assembly scaffold. In 2017, Henning-Knechtel et al. developed a DNA-guided assembly strategy to construct hybrid nanopores by using DNA-conjugated αHL monomers which can corral on circular DNA nanostructures (Figure 2d).[112] Unlike native αHL monomers that tend to form homogeneous heptameric αHL pores, the newly developed DNA-guided assembly led to hybrid nanopores of twelve, twenty and twenty-six subunits, which showed size-dependent electrical conductance.

A similar strategy to produce hybrid nanopores was pursued by assembling α-helical peptides from the polysaccharide transporter Wza, as reported by Spruijt et al.[113] The DNA-guided multimerisation harnessed a modular DNA scaffold formed of short oligonucleotides that hybridised to complementary oligonucleotides conjugated to Wza peptide monomers. This design caused the peptides to assemble into a stable, membrane-puncturing channel composed of eight peptide subunits (Figure 2e). However, despite the modularity of the scaffold, the approach did not yield nanopores with more than eight peptide subunits.

The DNA-guided strategy to create larger peptide pores was expanded by Fennouri et al. via the fabrication of a defined multimeric pore (Figure 2f).[114] The multimer pore was assembled from the peptide ceratotoxin A (CtXa), which naturally oligomerises on membrane surfaces to form random multimers. To achieve defined composition, a wheel-shaped DNA scaffold was prepared to hybridise with DNA-conjugated peptides. Stable assemblies with four, eight and twelvemer peptides yielded pores with larger lumens and defined conductance states. Additionally, the

DNA scaffold was equipped with cholesterol modifications which eased membrane insertion of the peptide pore.

Large DNA origami structures were also used as structural templates to arrange the subunit position within tetrameric Kir3K$^+$ channels, as realised by Kuokawa et al.[115] Subunit Kir3K$^+$ channel proteins were engineered to carry zinc finger proteins (ZFP) which are recognised by the origami scaffold with cognate ZPF binding sites. Adding a DNA origami nanostructure with four distal binding sites elicited a threefold increase in the current activity of the K$^+$ channel in HEK293T cells, indicating that the template changed the position or orientation of the protein subunits in the membrane channel.

Another approach to form even bigger pores was realised by using a circular DNA origami ring to corral up to 48 copies of the bacterial toxin pneumolysin, which readily formed a channel with an inner diameter of 22 nm.[116] This DNA-protein hybrid pore facilitated the exchange of molecules between liposomes and the outer environment. Controlled transport was then achieved by specifically decorating the DNA ring with disordered nucleoporin proteins.

3. DNA-functionalised solid-state nanopores

3.1. Pores modified with oligonucleotides

The properties of solid-state nanopores can be improved by functionalisation with DNA oligonucleotides. DNA modifications address issues of inconsistent lumen geometry and lack of ligand binding and achieve controlled structural and functional modulations of the pore. The modifications are installed by taking advantage of commercially available DNA strands and predictable secondary DNA structures, as well as the ability of DNA to mimic features of biological pores, such as ligand recognition or gating between open and closed states.

Tethering DNA oligonucleotides to the walls of solid-state nanopores has helped mimic the characteristic current rectification of biological nanopores. In rectifying pores, changes in the polarity applied voltage alter the conductance profile, which is often caused by physical movement of flexible parts within a narrow lumen region of the pore (Figure 3a).[117,118] Thiol-tagged oligonucleotides of varying lengths were conjugated into large conical gold nanopores with aperture sizes of 5 nm to 60 nm, resulting in nanopores demonstrating voltage-dependence conductance. The rectifi-

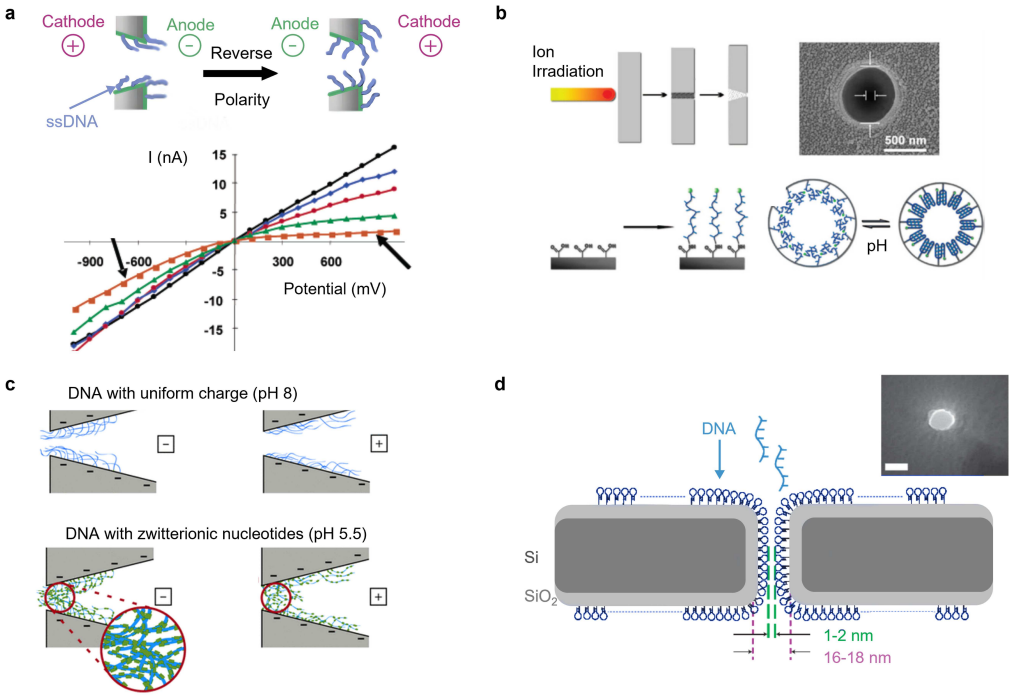

Figure 3. DNA-modified solid-state nanopores. a) A DNA-modified conical solid-state nanopore with DNA oligonucleotides grafted at the pore wall. The oligonucleotides are electrophoretically re-orientated under the applied voltage, yielding controlled current rectification depending on the voltage sign and magnitude. Current-voltage curves are shown for the undecorated pore (black), and the pore modified with oligonucleotides of 12 (blue), 15 (red), 30 (green) and 45 (orange) nucleotides in length. Adapted with permission from Ref. [118], Copyright 2004 American Chemical Society. b) A DNA-modified solid-state pore gated by a pH-responsive conformational switch of DNA *i*-motif strands (blue) attached at the pore walls. Adapted with permission from Ref. [119], Copyright 2008 American Chemical Society. c) A DNA modified solid-state nanopore showing voltage and pH-dependent gating, caused by the electrophoretically induced re-orientation of the DNA strands within the pore lumen, and the formation of pH-induced and electrostatically mediated network of DNA strands. Adapted with permission from Ref. [122], Copyright 2014 American Chemical Society. d) A DNA-hairpin-modified solid-state nanopore for the selective blockage and translocation of target DNA molecules. Adapted with permission from Ref. [123], Copyright 2007 Nature Publishing Group.

cation was caused by the electrophoretically induced reorientation of the DNA strands within the pore lumen as the membrane potential was switched in polarity.

Another property of biological nanopores, responsiveness to external pH, was re-created by grafting the solid-state pore lumen with DNA oligonucleotides of the pH-responsive i-motif sequences. At pH 4.5, the highly structured DNA oligonucleotides reduced the diameter of the pore, but upon exposure to neutral pH, the structures relaxed which increased the lumen size and channel conductance (Figure 3b).[119] In a similar manner, a G-quadruplex-forming sequence was also used to achieve regulation of conductance states in response to potassium concentrations, thereby mimicking the function of biological potassium channels.[120] In a further step, a synthetic route replicated the multi-stimuli responsiveness of potassium channels which are gated by the applied voltage and environmental salt concentration.[121] The multi-stimuli reactivity was successfully achieved in the Siwy group by conjugating DNA oligonucleotides to conical polymeric solid-state nanopores. Upon application of voltage the oligonucleotides altered their orientation in the pore which changed the pore's luminal diameter (Figure 3c).[122] The channel was also responsive to pH. Low pH protonated several nucleobases in the DNA oligonucleotides which—by electrostatic attraction to the negatively charged DNA backbone—resulted in the formation of a dense biopolymer meshwork and a lowering of the pore conductance (Figure 3c).

The introduction of a DNA coating within a solid-state nanopore was also employed to achieve selectivity in analyte recognition. By applying multiple DNA hairpin loops, the walls of the pore were able to selectively interact with analytes of complementary sequence. The highly specific base-pairing interactions of DNA enabled precise detection of mis-matches between the two oligonucleotides (Figure 3d).[123] Modification of solid-state pores is also possible with non-nucleic acid polymers. As one example, a Si_3N_4 solid-state nanopore was modified with peptides to control the pore lumen hydrophobicity and help detect gold nanoparticles.[124]

Alongside pH-dependent gating, oligonucleotide conjugation enabled the generation of ligand-responsive solid-state nanopores. Glass capillary nanopores with conjugated oligonucleotides were used to detect complementary DNA strands via hybridisation to detect single-base mismatches,[125] similar to the DNA-modified αHL.[105] By replacing unstructured oligonucleotides conjugated to a solid-state nanopore with folded DNA aptamers, the range of recognisable ligands was drastically expanded. The sensitivity of this technique was demonstrated by discrimination between human alpha and gamma thrombin by aptamer-equipped solid-state nanopores.[126]

Taking advantage of large lumen size, solid-state pores have furthermore been modified with complex hybrid DNA nanostructures. This research was motivated to overcome the poor signal and geometric inconsistencies within the lumen of nanopores. By electrophoretically driving a geometrically consistent protein pore with an attached negatively charged DNA oligonucleotide into a pre-formed solid-state pore, the signal was improved.[127] However, biosensing abilities were limited by the limited size range of the protein pore.

3.2. Solid-state pores functionalised with DNA nanostructures

DNA nanotechnology has enabled the de novo design and fabrication of DNA nanopores.[100] Creating custom-designed pores relies on building designed structures of larger dimensions than protein pores. Forming wide DNA nanopores also benefits from the ease of predicting DNA duplex formation as well as the larger nucleotide size, when compared to protein folding and amino acids, respectively.[128]

The first design of a funnel-shaped DNA origami nanopore featuring a 7.5 nm wide constriction was realised by Bell et al.[129] This large hollow DNA nanostructure was inserted into the lumen of a solid-state pore and helped detect DNA analytes. The inherent charge of the DNA structure enabled electrophoretic docking into the lumen of a solid-state pore. The docking efficiency was found to be increased by adding an extended single-stranded tail to help electrophoretically thread the DNA pore into a solid-state pore (Figure 4a).

In independent parallel work, Wei et al. designed DNA origami plates with 6 nm thickness and a central opening of varying size (Figure 4b).[130] The docking of the DNA plate structures over solid-state apertures was investigated. The relative conductance of was reduced for smaller openings within the DNA plate. The size-customised DNA origami structures also acted as size-selective filters by hindering the translocation of molecules exceeding the opening diameter. Challenges of DNA origami plates include the high ionic leakage which is mainly attributed to ion permeation pathways through the lattice of DNA helices. This leads to considerable ionic current noise compared to non-hybrid solid-state pores and impedes single-molecule sensing. In addition, the charged nature of the DNA structures results in deformations under high voltage.[133]

In another docking approach, a DNA nanostructure was created to mimic the large biological nuclear pore complex. Ketterer et al. docked into a solid-state pore a 57 nm-wide DNA origami ring conjugated with the nuclear pore complex peptides (Figure 4c).[131] This biomimetic structure enabled the investigation of essential transport properties of the otherwise difficult-to-explore large and structurally intricate biological nuclear pore complex.

Recently, a DNA origami sphere -docked onto a solid-state pore- formed an electro-osmotic trap to capture and analyse proteins for hours with sub-millisecond resolution, as attained by Schmid et al.[134] The electro-osmotic flow was induced by the highly negatively charged nature of the DNA sphere which causes the flux of charge compensation cations and the surrounding water molecules. This electro-osmotic trap allowed the differentiation between size, shape and nucleotide-dependent conformation of proteins as shown with the protein Hsp90. While DNA origami structures have

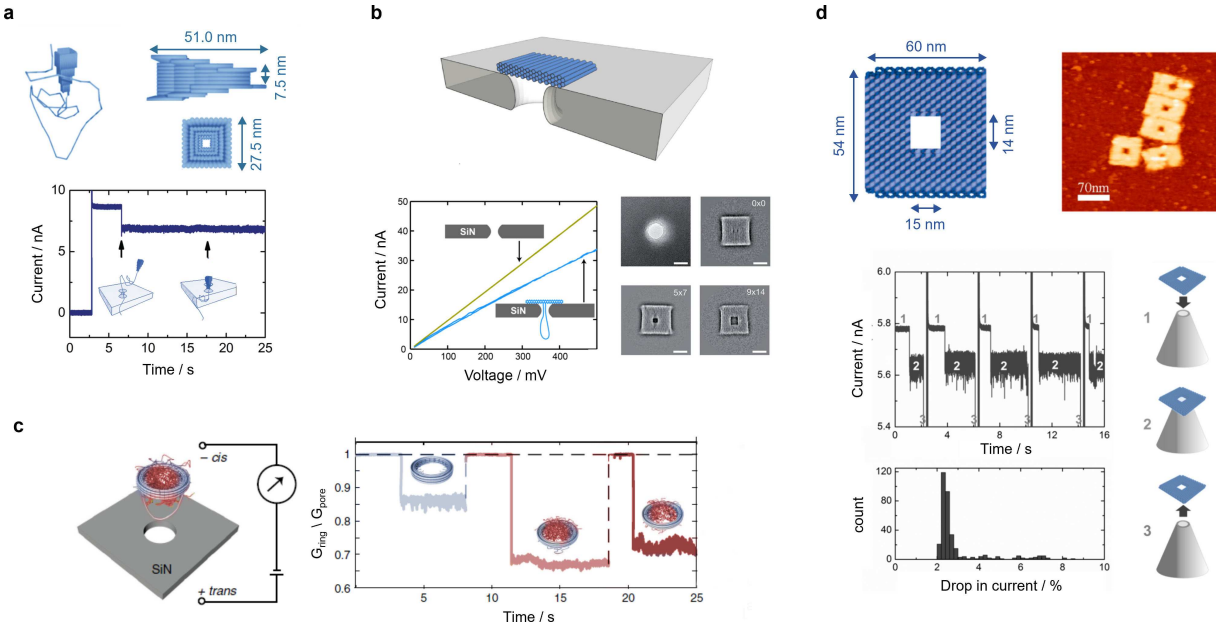

Figure 4. DNA origami nanopores positioned on and within solid-state nanopores. a) A hybrid pore formed by inserting a folded DNA origami funnel (top) into a solid-state pore (below). The insertion of the funnel into the pore is guided by the threading of an attached DNA double strand. Successful insertion of the funnel into the solid-state pore is detected by a current blockage in a single-channel current trace (bottom). Adapted with permission from Ref. [129], Copyright 2012 American Chemical Society. b) A rectangular DNA nanoplate docked on a SiN solid-state nanopore. The electrophoretically induced docking of the DNA nanopore is registered by a change in the current-voltage curve. Transmissing electron microscopy images show top-down views of the solid-state pore and assembled DNA plates with increasing opening sizes. Adapted with permission from Ref. [130], Copyright 2012 Wiley-VCH. c) A biomimetic nuclear pore complex, created from a DNA origami ring, whose lumen is decorated with yeast FG-Nup peptides (left). The complex was docked onto a solid state nanopore thereby causing a decrease in conductance in the conductance trace (right). The conductance decrease is proportional to whether the structure was undecorated (blue) or decorated with the FG-Nup peptides (light red) or with a mutant peptide (dark red). Adapted with permission from Ref. [131], Copyright 2018 Nature Publishing Group. d) Schematics of a DNA origami nanoplate (top, left) and atomic force microscopy images showing the assembled structure (top, right). The DNA origami nanoplate can be reversibly trapped on and ejected from a glass nanocapillary, as shown by changes in the current traces (middle) and histogram (bottom). The numbering 1–3 corresponds to the steps of the process of trapping and ejection in a scheme (right). The histogram shows a 2.5 % drop in current for over 350 measured trapping events. Adapted with permission from Ref. [132], Copyright 2013 American Chemical Society.

found widespread use to fine-tune the dimensions of solid-state nanopores[132,135] (Figure 4d), a limitation is the need to apply a voltage to maintain docking of the structure at the pore entrance. Strengthening the association of the structure to the pore can be achieved via hydrophobic modifications. By decorating the DNA origami sphere with cholesterol-modified oligonucleotides, Wen et al. were able to overcome thermal fluctuations of the DNA origami sphere which limited the trapping of small particles.[136] The incorporation of hydrophobic modifications to DNA nanostructures is also used in the construction of spontaneously inserting membrane nanopores built entirely of DNA.

4. Self-assembled DNA membrane nanopores

DNA nanopores of highly defined structure can be inserted into lipid bilayers and related semifluid membrane for applications in biological and biophysical research and sensing. To achieve membrane binding and puncturing, DNA nanopore are equipped with hydrophobic modifications at selected sites within the designed nanostructure. Pioneering work in the field of membrane-spanning DNA nanopores was performed by Langecker et al. who, inspired by the structure of αHL, designed a membrane-puncturing nanopore via DNA self-assembly (Figure 5a).[137] The DNA duplexes in the pore were arranged in a honeycomb lattice to form a large DNA origami extramembrane cap structure (Figure 5a). A central hollow 2 nm-wide lumen extended to the protruding membrane-puncturing channel (Figure 5a). Up to 46 cholesterol membrane anchors were attached to the structure to enable binding onto lipid membranes and puncturing of the bilayer (Figure 5a).

In independent and parallel work by Burns et al., a membrane-spanning DNA nanopore was fabricated with a core of six hexagonally arranged duplexes enclosing a 2 nm lumen.[138] The pore was assembled from just 14 DNA strands. Membrane anchoring of the 15 nm long duplex bundle was achieved by a hydrophobic belt composed of neutrally charged phosphorothioate-ethyl (PPT) which were installed at corresponding sections of the DNA backbone (Figure 5b). In other work, the hydrophobic belt was replaced with two porphyrin-based tetraphenyl-porphyrin (TPP) tags[139] as alternative membrane anchors for a six-helix-bundle DNA pore (Figure 5c). In addition to functioning as anchors, TPP exhibits fluorescence emission, which

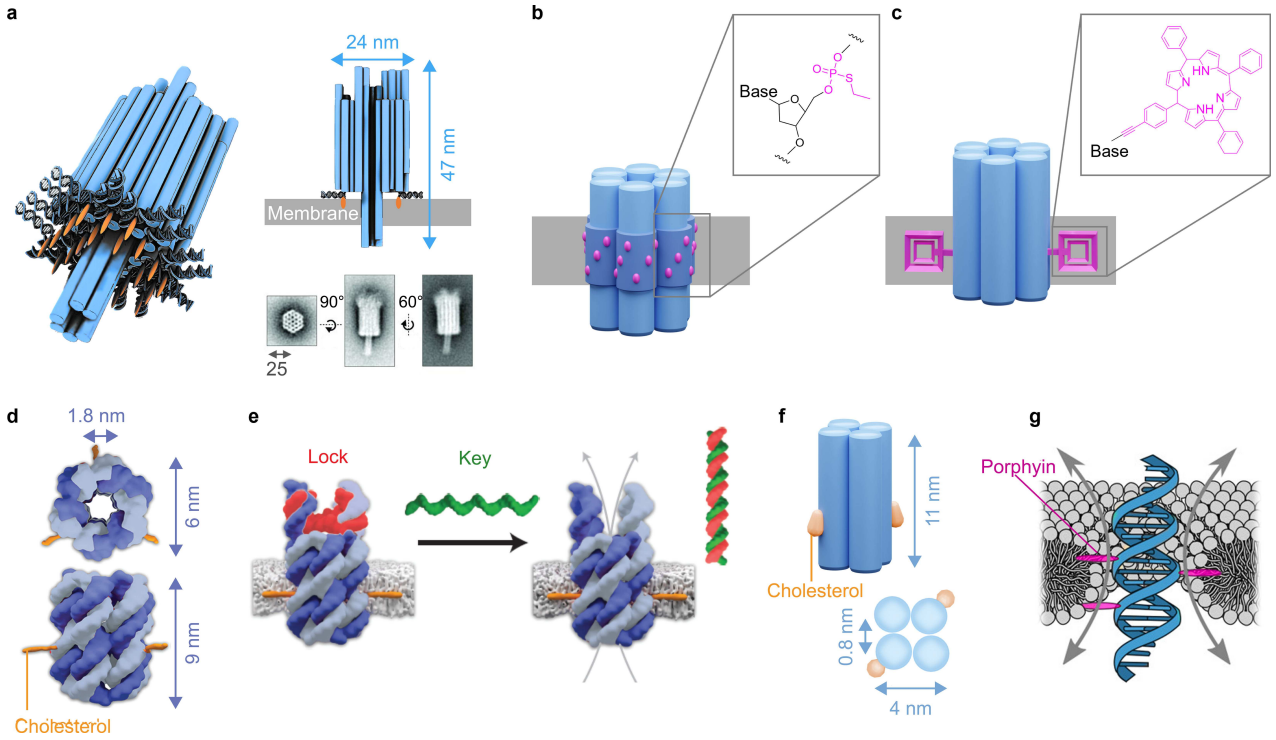

Figure 5. Bilayer-spanning DNA nanopores with narrow lumens of up to 2 nm. a) A large DNA origami channel functionalised with cholesterol anchors (orange) to insert into lipid bilayer. TEM images of the DNA pore at different angles. Adapted with permission from Ref. [137], Copyright 2012 American Association for the Advancement of Science b, c) Six-helix-bundle DNA nanopores carrying b) phosphorothioate-ethyl[138] and c) tetraphenylporphyrin anchors[139] for membrane insertion. Adapted with permission from Ref. [138] and Ref. [139], Copyright 2012 American Chemical Society and Wiley-VCH 2013. d), e) A six-helix-bundle nanopore with 1.8 nm lumen, holding d) three cholesterol anchors for membrane insertion and e) a modified version that carries a lock strand (red) which can be removed by competitive hybridisation with a key strand (green) to open up the channel. Adapted with permission from Ref. [145], Copyright 2016 Nature Publishing Group. f) A minimal DNA pore composed of 4 duplexes enclosing a lumen of 0.8 nm. Adapted with permission from Ref. [146], Copyright 2015 American Chemical Society. g) Membrane placement of the single DNA duplex forms a toroidal lipid channel with a gap between the outer surface of the DNA duplex and the membrane surface. Adapted with permission from Ref. [147], Copyright 2016 American Chemical Society.

was used to verify the pore's membrane insertion as porphyrin fluorescence shifts upon a change into the hydrophobic membrane environment. The hydrophobic anchors were also moved to one pore terminus for easier membrane insertion and these DNA pores were found cytotoxic as the incubation of the pore with cervical cancer HeLa cells significantly reduced the cell viability.[140] The influence of the exact position of cholesterol modifications on lipid bilayer interaction was tested on a cubic DNA scaffold structure by Chidchob et al.[141] By specifically designing the positions of the hydrophobic interactions, it was possible to guide peripheral anchoring and conformational switching of the nanopore. Furthermore, this cubic pore represents the first DNA pore with hollow walls where only one quarter of wall surfaces was covered by DNA. Interaction of DNA nanopores with lipid bilayers was further elucidated with the six-helix bundle pore, revealing a two-step mechanism consisting of a rapid membrane tethering followed by a slow reorientation of the pore resulting in membrane punctuation.[142,143] These DNA nanopores could also insert into synthetic membrane vesicles to form hybrid nanocontainers.[144]

Another DNA pore of the six-helix-bundle type was designed by using only six interconnected DNA strands (Figure 5d).[145] It was observed that the pore switched between an open, high-conductance and a closed, low-conductance state, depending on the magnitude of the applied voltage. This changes reflected the electrophoretic movement of the negatively charged pore wall sections, which was also observed in the TTP-tagged pore.[146] The design of the six-helix bundle pore was further advanced by equipping it with a nanomechanical gate to control the flow of molecules across the membrane (Figure 5e).[145] Closing of the lumen and hindrance of the flux was reached by binding a lid DNA strand to two single-stranded DNA overhangs on top of the pore. The addition of a key DNA strand removed the lid by hybridising and unzipping the lid strand and resulting in an opened pore. Single-channel current recordings confirmed low permeability of the closed pore (0.7 nS) but significantly higher upon the addition of the key strand (1.6 nS). Furthermore, this pore acted as a charge-selective filter, allowing 130-fold quicker passage of small molecule sulforhodamine B carrying one positive and two negative charges compared to a triple negatively charged indicator molecule carboxy-fluorescein. The transport principles and

kinetics of small-molecule transport through the lumen of the six-helix bundle pore was examined using simultaneous readout of hundreds of individual pores and molecular dynamic simulation.[147] This analysis revealed that the pore's selectivity in transport depends on steric and electrostatic factors but also the composition of the lipid bilayer in which the pore is embedded. Recently, the repertoire of gated six-helix-bundle pores has been expanded for external triggers such as heat,[148] protein binding,[149] light[150] and ATP binding.[151] Six-helical bundle DNA pores were also shown to have clinical application, puncturing live cell membranes and transporting anti-tumour drugs.[152] The assembly pathway of the six-helix bundle pore was recently monitored by ion mobility mass spectrometry,[153] while their structural conformations have been investigated using cryo-electron microscopy and molecular dynamics simulations.[154–156]

The dimensions of DNA pore structures were further reduced by Göpfrich et al., with the design of a DNA channel comprising solely four duplexes that enclosed a subnanometer lumen (Figure 5f).[157] Using the DNA tile design, the DNA channel was built out of 8 interconnected DNA strands enclosing a lumen of approximately 0.8 nm. The incorporation of cholesterol modifications and Cy3-tags allowed membrane interaction and fluorescent visualisation. In other work by Lanphere et al.[158] it was possible to control the formation of four-duplex DNA pores in membranes from two halves. The membrane-bound halves were assembly-inactive due to lock strands. But these could be unzipped by key strands leading to assembly into hollow channels for transmembrane transport.

Göpfrich et al. designed so far the smallest pore, simply consisting of one single 5 nm long DNA duplex anchored to the membrane with porphyrin tags (Figure 5g).[159] While in previous DNA pores the central water-filled channel was enclosed by several DNA duplexes, the minimal pore featured a thin water-filled perimeter between the outer surface of the central duplex and the surrounding lipid bilayer membrane. The formation of the toroidal pore was confirmed by demonstrating the minuscule passage of ions through the gaps between the DNA and the lipid bilayer and by analysis with molecular dynamics simulations. The torodial shape of the membrane -as induced by the anchor-modified pore- was also used to mimick the function of the flippase enzyme which facilitates transport of lipids between the two bilayer leaflets, as shown for four-duplex pore.[160] While this small gap between DNA duplexes and lipid bilayers is facilitated by the few cholesterol or porphyrin anchors, a hydrophobic belt formed by alkylated PPT anchors resulted in a tight seal with the surrounding membrane.[155,161]

The fabrication of a membrane-spanning DNA pore with a larger lumen was first reported by Krishnan et al. who introduced a DNA origami pore enclosing a 4.2 nm × 4.2 nm lumen (Figure 6a).[162] This T-shaped pore consisted of a double-duplex layered cap and a hollow central stem, as well as 57 hydrophobic tocopherol membrane anchors spread around the bottom side of the cap region. Membrane association was alternatively achieved with biotinylated lipids and streptavidin bridges to biotinylated anchors at the pore's underside. The wide lumen of the T-shape pore allowed translocation of ssDNA strands of up to 527 base-pairs in length.

An artificial funnel-shaped DNA pore with an even wider lumen of 6 nm × 6 nm was fabricated by Göpfrich et al. (Figure 6b).[163] Confocal imaging and ionic current recordings revealed that the pore can insert into bilayers via the incorporation of 19 cholesterol tags and show high conductance caused by the wide funnel lumen. In another separate study, a funnel-shaped DNA origami pore with a 7.5 nm × 7.5 nm wide lumen demonstrated the capability of translocating folded proteins (Figure 6c) as reported by Diederichs et al.[164] The molecular transport through the pore was confirmed via spectroscopic and electrical readout revealing a 20-fold speed increase under electrophoresis compared to diffusion. A diffusion of up to 66 molecules per second was observed. The pore acted as a size-specific filter for proteins, only allowing proteins with a diameter below the lumen size to translocate.

To complement the static pores, a dynamic design was introduced by Thomsen et al. with a dynamic hexagonal-based DNA origami pore of 9 nm lumen width and 32 nm height (Figure 6d). [165] The pore featured three nano-mechanical flaps which, upon strand displacement, were opened to reveal hydrophobic moieties for membrane binding. Actuation-based membrane insertion was confirmed by binding assays with membrane vesicles. The size-specific translocation of different molecular cargos was confirmed.

A large reversibly gated DNA pore with the ability to control the transport of folded proteins across bilayers was introduced by Dey et al. (Figure 6e).[166] The pore features an extramembrane DNA origami plate with a central square-shaped 416 nm^2 large hole which was equipped with a hinge-attached nanomechanical lid. The DNA pore also featured a membrane-spanning channel. The pore could be reversibly opened and closed via a lock-and-key mechanism to control the transport of proteins across bilayer membranes.

Another de novo rational design strategy was developed by Xing et al. to build DNA origami nanopores of tunable pore shapes and sizes with a lumen diameter of up to tens of nanometres (Figure 6f).[104] The pores were not designed via the traditional route of bundling all DNA duplexes in a parallel fashion to puncture the bilayer. Rather the duplexes were assembled into modular units that were linked into tunable shapes including triangles (Figure 6f), squares (Figure 1e), pentagons and hexagons. All pore variants were composed of an extramembrane cap and a membrane-spanning channel, and DNA duplexes were lying parallel to the membranes. By taking advantage of the large lumen size and precise modification of the pore walls with receptors, the pores allowed direct label-free sensing of protein analytes, such as streptavidin and the SARS-CoV-2 antibody (Figure 6f).[104]

Increasing the length of pores instead of lumen diameter is a research venture pursued by Schulman's group by creating multiple micrometre-long DNA nanochannels. The DNA nanochannels were self-assembled from DNA double crossover tiles[168] enclosing a 7 nm-wide channel lumen

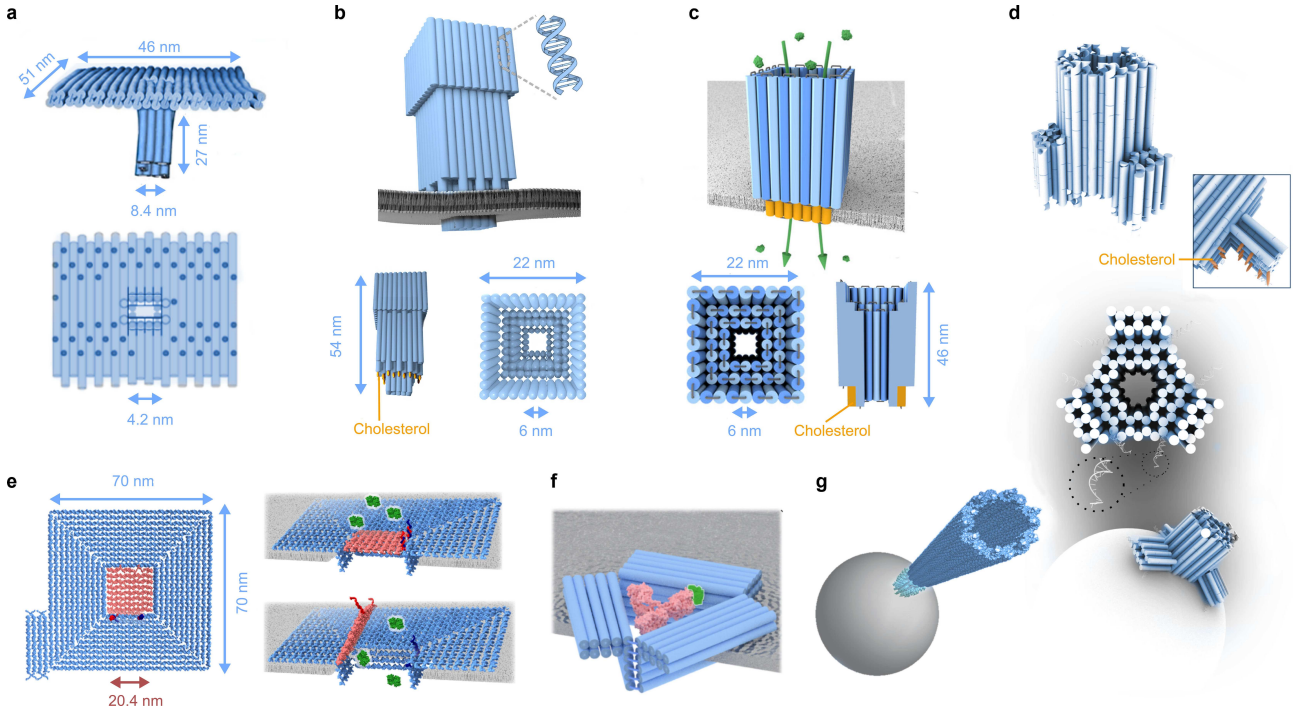

Figure 6. Large DNA origami nanopores with lumen sizes wider than 2 nm. a) A DNA origami nanopore with a lumen width of 4 nm allows translocation of single- and double-stranded DNA molecules. Adapted with permission from Ref. [162], Copyright 2016 Nature Publishing Group. b) A funnel-shaped DNA origami nanopore with a lumen width of 6 nm at its narrowest position, inserted into a lipid bilayer. Adapted with permission from Ref. [163], Copyright 2016 American Chemical Society. c) A 6 nm-wide lumen-spanning DNA origami pore in square-lattice design facilitating the translocation of folded proteins (green). Adapted with permission from Ref. [164], Copyright 2019 Nature Publishing Group. d) A honeycomb-lattice pore enclosing a 9 nm lumen and equipped with programable flaps of cholesterol anchors for controllable membrane pore insertion. Adapted with permission from Ref. [165], Copyright 2019 Nature Publishing Group. e) A DNA origami nanopore with a 20.4 nm × 20.4 nm-wide lumen is equipped with a gated lid. Upon the addition of key strands (not shown), the lid can be opened and closed to control the transmembrane flux of protein cargo (green). Adapted with permission from Ref. [166], Copyright 2022 Nature Publishing Group. f) A shape- and size-tuneable nanopore design illustrated by a 20 nm triangular pore. The channel lumen is functionalised with a receptor (green, receptor binding domain of SARS-CoV-2) to specifically detect the cognate protein (pink, antibody). Adapted with permission from Ref. [104], Copyright 2022 Nature Publishing Group. g) Scheme of a micrometre-long DNA nanochannel inserted via its cholesterol-modified terminus to the membrane of a bilayer vesicle. Adapted with permission from Ref. [167], Copyright 2022 American Association for the Advancement of Science.

(Figure 6g). This approach acts as a self-healing mechanism[169] and forms flow networks connecting multicellular compartments.[170] Controlled migration of dye across the DNA nanochannel was demonstrated with control structures where one channel opening was capped.[167]

5. Summary and Outlook

In this review we have surveyed recent advances of functional nanopore systems enabled by DNA modification and DNA nanotechnology. The use of DNA expands the structural and functional repertoire of existing nanopores and is the basis for a separate class of nanopores. DNA confers new properties to existing and new pores in terms of specific molecular interaction, shape and size, and nanomechanical changes, thereby overcoming shortcomings of existing nanopore systems. In the following, the advantages and limitations of the DNA-led approaches are summarised, along with possible future developments.

5.1. Integrating stimulus response by tethering DNA strands to protein and solid-state pores

This approach adds functionality not easily accessible by the pore material but operates within the constraints of DNA; only analytes and stimuli responsiveness allowable by DNA can be used. Similarly, the introduced functionality cannot considerably alter pore dimensions and shape. One challenge is to add DNA strands in defined numbers and positions to the walls of solid-state pores.

5.2. DNA nanostructures as structural templates to guide the assembly of pore-forming peptides/proteins

This route yields protein pores of defined composition and shape not accessible by a non-templated assembly of component proteins and peptides. As a requirement, peptides and proteins have to be engineered to carry a DNA strand that interacts with the template; this is usually not an issue. The pore shape accessible by the route is currently circular but may in future be tuned with other origami

structures. A limitation for several biological applications is that the hybrid DNA protein/peptide pores are fabricated in a test tube rather than being produced by the cell, something which is routinely achieved by genetic engineering of proteins.

5.3. DNA origami structures to tune the lumen structure and function of solid-state nanopores

This route places DNA origami plates on top of solid-state pores or inserts DNA nanofunnels into the pore lumen. Thereby, the lumen shape and width are tuned. Furthermore, nanomechanical changes can be introduced to control pore transport properties. As a drawback, positioning DNA origami structures into solid-state pores usually does not achieve a tight seal which reduces the resolution of electrical recordings of the DNA structures.

5.4. De novo designed DNA nanopores to puncture lipid bilayers

The strategy offers nanopores with well-defined dimensions and designed structural dynamic properties, but also achieves novel functions, such as controlled molecular transport and sensing capabilities. Pore shape and dimensions are widely tuneable. Two limitations are the greater structural flexibility of DNA structures compared to protein assemblies. Another is the highly negatively charged nature of DNA which can lead to electrophoretically induced changes in pore shape at high transmembrane potentials. The charged nature also lowers the membrane insertion efficiency of DNA nanopores. These points can be addressed by chemical modifications to the DNA backbone.

5.5. Other approaches and future developments

Rather than using DNA to modify or form a pore, DNA tethering can be applied in other ways to benefit nanopore sensing. For example, attaching DNA to a peptide strand has led to a new approach in single molecule peptide sequencing with nanopores.[18,171] This route takes advantage of existing DNA sequencing technology of nanopores. The DNA part of the peptide-DNA conjugate is recognised by the molecular sequencing machinery so that the movement of the tethered peptide across the nanopore's sensing section is controlled to allow reading of the peptide sequence. Another approach is to use DNA nanotechnology to create carriers that specifically bind proteins and facilitate sensing. This strategy can rely on analyte recognising aptamers and nanocarriers[172–175] that also encode information to achieve multiplex sensing.[176] The DNA carriers have specific binding sites and barcode sequences, which can identify the presence of a target via a single current signal, when the corresponding carrier passes through a nanopore. This approach has been used to sense proteins at nanomolar concentrations,[177] detect antibodies,[178] and perform real-time kinetic screening.[179] Furthermore, DNA nanocarriers allow the identification of RNA isoforms by specifically binding target RNA followed by single-molecule pore sensing.[180] Future developments on DNA modification and DNA nanotechnology and nanopore techniques could yield advanced analytical platforms[11] with precisely tuned pores to detect molecular analytes, single-molecule research tools for ligand-receptor binding[104] and chemical/enzymatic reactions,[181] and biomimetic nanostructures[182] to replicate transmembrane flux,[154] signal transduction, and molecular motors.[183]

Conflict of Interest

Y.X and S.H. are inventors of patents on DNA origami nanopores which have been licensed to Oxford Nanopore Technologies plc.

Keywords: DNA · DNA Nanotechnology · Nanopore · Nanostructure · Self-Assembly

[1] E. Gouaux, R. MacKinnon, *Science* **2005**, *310*, 1461–1465.
[2] B. Alberts, A. Johnson, J. Lewis, M. Raff, K. Roberts, P. Walter, *Molecular Biology of the Cell*, 4th ed., Garland Science, New York, **2002**.
[3] J. D. Rioux, A. K. Abbas, *Nature* **2005**, *435*, 584–589.
[4] S. Majd, E. C. Yusko, Y. N. Billeh, M. X. Macrae, J. Yang, M. Mayer, *Curr. Opin. Biotechnol.* **2010**, *21*, 439.
[5] G. Huang, A. Voet, G. Maglia, *Nat. Commun.* **2019**, *10*, 835.
[6] H. Ouldali, K. Sarthak, T. Ensslen, F. Piguet, P. Manivet, J. Pelta, J. C. Behrends, A. Aksimentiev, A. Oukhaled, *Nat. Biotechnol.* **2020**, *38*, 176–181.
[7] C. Cao, Y. L. Ying, Z. L. Hu, D. F. Liao, H. Tian, Y. T. Long, *Nat. Nanotechnol.* **2016**, *11*, 713–718.
[8] D. Rotem, L. Jayasinghe, M. Salichou, H. Bayley, *J. Am. Chem. Soc.* **2012**, *134*, 2781–2787.
[9] A. K. Thakur, L. Movileanu, *Nat. Biotechnol.* **2019**, *37*, 96–101.
[10] N. S. Galenkamp, A. Biesemans, G. Maglia, *Nat. Chem.* **2020**, *12*, 481–488.
[11] Y. L. Ying, Z. L. Hu, S. Zhang, Y. Qing, A. Fragasso, G. Maglia, A. Meller, H. Bayley, C. Dekker, Y. T. Long, *Nat. Nanotechnol.* **2022**, *17*, 1136–1146.
[12] S. Howorka, Z. Siwy, *Chem. Soc. Rev.* **2009**, *38*, 2360–2384.
[13] J. J. Kasianowicz, E. Brandin, D. Branton, D. W. Deamer, *Proc. Natl. Acad. Sci. USA* **1996**, *93*, 13770–13773.
[14] H. Bayley, P. S. Cremer, *Nature.* **2001**, *413*, 226-230.
[15] L. Movileanu, S. Howorka, O. Braha, H. Bayley, *Nat. Biotechnol.* **2000**, *18*, 1091–1095.
[16] I. Nir, D. Huttner, A. Meller, *Biophys. J.* **2015**, *108*, 2340–2349.
[17] L. Movileanu, J. P. Schmittschmitt, J. M. Scholtz, H. Bayley, *Biophys. J.* **2005**, *89*, 1030–1045.
[18] H. Brinkerhoff, A. S. W. Kang, J. Liu, A. Aksimentiev, C. Dekker, *Science* **2021**, *374*, 1509–1513.
[19] L. Yu, X. Kang, F. Li, B. Mehrafrooz, A. Makhamreh, A. Fallahi, J. C. Foster, A. Aksimentiev, M. Chen, M. Wanunu, *Nat. Biotechnol.* **2023**, https://doi.org/10.1038/s41587-022-01598-3.
[20] M. Wanunu, T. Dadosh, V. Ray, J. Jin, L. McReynolds, M. Drndić, *Nat. Nanotechnol.* **2010**, *5*, 807–814.

[21] J. Clarke, H.-C. Wu, L. Jayasinghe, A. Patel, S. Reid, H. Bayley, *Nat. Nanotechnol.* **2009**, *4*, 265–270.
[22] G. M. Cherf, K. R. Lieberman, H. Rashid, C. E. Lam, K. Karplus, M. Akeson, *Nat. Biotechnol.* **2012**, *30*, 344–348.
[23] E. A. Manrao, I. M. Derrington, A. H. Laszlo, K. W. Langford, M. K. Hopper, N. Gillgren, M. Pavlenok, M. Niederweis, J. H. Gundlach, *Nat. Biotechnol.* **2012**, *30*, 349–353.
[24] J. Quick, N. J. Loman, S. Duraffour, J. T. Simpson, E. Severi, L. Cowley, J. A. Bore, R. Koundouno, G. Dudas, A. Mikhail, N. Ouédraogo, B. Afrough, A. Bah, J. H. J. Baum, B. Becker-Ziaja, J. P. Boettcher, M. Cabeza-Cabrerizo, Á. Camino-Sánchez, L. L. Carter, J. Doerrbecker, T. Enkirch, I. Garciá-Dorival, N. Hetzelt, J. Hinzmann, T. Holm, L. E. Kafetzopoulou, M. Koropogui, A. Kosgey, E. Kuisma, C. H. Logue, A. Mazzarelli, S. Meisel, M. Mertens, J. Michel, D. Ngabo, K. Nitzsche, E. Pallasch, L. V. Patrono, J. Portmann, J. G. Repits, N. Y. Rickett, A. Sachse, K. Singethan, I. Vitoriano, R. L. Yemanaberhan, E. G. Zekeng, T. Racine, A. Bello, A. A. Sall, O. Faye, O. Faye, N. Magassouba, C. V. Williams, V. Amburgey, L. Winona, E. Davis, J. Gerlach, F. Washington, V. Monteil, M. Jourdain, M. Bererd, A. Camara, H. Somlare, A. Camara, M. Gerard, G. Bado, B. Baillet, D. Delaune, K. Y. Nebie, A. Diarra, Y. Savane, R. B. Pallawo, G. J. Gutierrez, N. Milhano, I. Roger, C. J. Williams, F. Yattara, K. Lewandowski, J. Taylor, P. Rachwal, D. J. Turner, G. Pollakis, J. A. Hiscox, D. A. Matthews, M. K. O'Shea, A. M. D. Johnston, D. Wilson, E. Hutley, E. Smit, A. Di Caro, R. Wolfel, K. Stoecker, E. Fleischmann, M. Gabriel, S. A. Weller, L. Koivogui, B. Diallo, S. Keita, A. Rambaut, P. Formenty, S. Gunther, M. W. Carroll, *Nature* **2016**, *530*, 228–232.
[25] M. Jain, S. Koren, K. H. Miga, J. Quick, A. C. Rand, T. A. Sasani, J. R. Tyson, A. D. Beggs, A. T. Dilthey, I. T. Fiddes, S. Malla, H. Marriott, T. Nieto, J. O'Grady, H. E. Olsen, B. S. Pedersen, A. Rhie, H. Richardson, A. R. Quinlan, T. P. Snutch, L. Tee, B. Paten, A. M. Phillippy, J. T. Simpson, N. J. Loman, M. Loose, *Nat. Biotechnol.* **2018**, *36*, 338–345.
[26] S. E. Van der Verren, N. Van Gerven, W. Jonckheere, R. Hambley, P. Singh, J. Kilgour, M. Jordan, E. J. Wallace, L. Jayasinghe, H. Remaut, *Nat. Biotechnol.* **2020**, *38*, 1415–1420.
[27] L. Song, M. R. Hobaugh, C. Shustak, S. Cheley, *Science* **1996**, *274*, 1859–1866.
[28] M. Akeson, D. Branton, J. J. Kasianowicz, E. Brandin, D. W. Deamer, *Biophys. J.* **1999**, *77*, 3227–3233.
[29] M. Faller, M. Niederweis, G. E. Schulz, *Science* **2004**, *303*, 1189–1192.
[30] P. Goyal, P. V. Krasteva, N. Van Gerven, F. Gubellini, I. Van Den Broeck, A. Troupiotis-Tsaïlaki, W. Jonckheere, G. Péhau-Arnaudet, J. S. Pinkner, M. R. Chapman, S. J. Hultgren, S. Howorka, R. Fronzes, H. Remaut, *Nature* **2014**, *516*, 250–253.
[31] J. E. Reiner, A. Balijepalli, J. W. F. Robertson, J. Campbell, J. Suehle, J. J. Kasianowicz, *Chem. Rev.* **2012**, *112*, 6431–6451.
[32] D. A. Doyle, J. M. Cabral, R. A. Pfuetzner, A. Kuo, J. M. Gulbis, S. L. Cohen, B. T. Chait, R. MacKinnon, *Science* **1998**, *280*, 69–77.
[33] M. T. Degiacomi, I. Iacovache, L. Pernot, M. Chami, M. Kudryashev, H. Stahlberg, F. G. Van Der Goot, M. Dal Peraro, *Nat. Chem. Biol.* **2013**, *9*, 623–629.
[34] G. Chang, R. H. Spencer, A. T. Lee, M. T. Barclay, D. C. Rees, *Science* **1998**, *282*, 2220–2226.
[35] A. D. Ferguson, E. Hofmann, J. W. Coulton, K. Diederichs, W. Welte, *Science* **1998**, *282*, 2215–2220.
[36] M. Mueller, U. Grauschopf, T. Maier, R. Glockshuber, N. Ban, *Nature* **2009**, *459*, 726–730.
[37] A. A. Simpson, Y. Tao, P. G. Leiman, M. O. Badasso, Y. He, P. J. Jardine, N. H. Olson, M. C. Morais, S. Grimes, D. L. Anderson, T. S. Baker, M. G. Rossmann, *Nature* **2000**, *408*, 745–750.
[38] L. Jayasinghe, E. J. Wallace, WO2012107778A3, **2017**.
[39] W. Jia, C. Hu, Y. Wang, Y. Gu, G. Qian, X. Du, L. Wang, Y. Liu, J. Cao, S. Zhang, S. Yan, P. Zhang, J. Ma, H. Y. Chen, S. Huang, *Nat. Commun.* **2021**, *12*, 5811.
[40] W. Jia, C. Hu, Y. Wang, Y. Liu, L. Wang, S. Zhang, Q. Zhu, Y. Gu, P. Zhang, J. Ma, H. Y. Chen, S. Huang, *ACS Nano* **2022**, *16*, 6615–6624.
[41] D. Stoddart, A. J. Heron, E. Mikhailova, G. Maglia, H. Bayley, *Proc. Natl. Acad. Sci. USA* **2009**, *106*, 7702–7707.
[42] B. Walker, J. Kasianowicz, M. Krishnasastry, H. Bayley, *Protein Eng. Des. Sel.* **1994**, *7*, 655–662.
[43] D. Stoddart, M. Ayub, L. Höfler, P. Raychaudhuri, J. W. Klingelhoefer, G. Maglia, A. Heron, H. Bayley, *Proc. Natl. Acad. Sci. USA* **2014**, *111*, 2425–2430.
[44] S. Koo, S. Cheley, H. Bayley, *ACS Cent. Sci.* **2019**, *5*, 629–639.
[45] B. Walker, H. Bayley, *Protein Eng. Des. Sel.* **1994**, *7*, 91–97.
[46] B. Walker, H. Bayley, *Protein Eng. Des. Sel.* **1995**, *8*, 491–495.
[47] X. Guan, L. Q. Gu, S. Cheley, O. Braha, H. Bayley, *ChemBioChem* **2005**, *6*, 1875–1881.
[48] M. Soskine, A. Biesemans, B. Moeyaert, S. Cheley, H. Bayley, G. Maglia, *Nano Lett.* **2012**, *12*, 4895–4900.
[49] G. Maglia, M. Henricus, R. Wyss, Q. Li, S. Cheley, H. Bayley, *Nano Lett.* **2009**, *9*, 3831–3836.
[50] M. M. Mohammad, R. Iyer, K. R. Howard, M. P. McPike, P. N. Borer, L. Movileanu, *J. Am. Chem. Soc.* **2012**, *134*, 9521–9531.
[51] J. M. Reimer, M. N. Aloise, P. M. Harrison, T. Martin Schmeing, *Nature* **2016**, *529*, 239–242.
[52] S. Krishnan, R. Satheesan, N. Puthumadathil, K. S. Kumar, P. Jayasree, K. R. Mahendran, *J. Am. Chem. Soc.* **2019**, *141*, 2949–2959.
[53] J. Montenegro, M. R. Ghadiri, J. R. Granja, *Acc. Chem. Res.* **2013**, *46*, 2955–2965.
[54] M. Mayer, J. Yang, *Acc. Chem. Res.* **2013**, *46*, 2998–3008.
[55] H. Tawfik, S. Puza, R. Seemann, J. B. Fleury, *Front. Cell Dev. Biol.* **2020**, *8*, 531229.
[56] B. A. Cornell, V. L. B. Braach-Maksvytis, L. G. King, P. D. J. Osman, B. Raguse, L. Wieczorek, R. J. Pace, *Nature* **1997**, *387*, 580–583.
[57] S. Howorka, *Nat. Nanotechnol.* **2017**, *12*, 619–630.
[58] A. R. Thomson, C. W. Wood, A. J. Burton, G. J. Bartlett, R. B. Sessions, R. L. Brady, D. N. Woolfson, *Science* **2014**, *346*, 485–488.
[59] M. W. Parker, F. Pattus, A. D. Tucker, D. Tsernoglou, S. J. Tilley, E. V. Orlova, R. J. Gilbert, P. W. Andrew, H. R. Saibil, *Cell* **2005**, *121*, 247–256.
[60] M. D. Peraro, F. G. Van Der Goot, *Nat. Rev. Microbiol.* **2016**, *14*, 77–92.
[61] T. X. Dang, E. M. Hotze, I. Rouiller, R. K. Tweten, E. M. Wilson-Kubalek, *J. Struct. Biol.* **2005**, *150*, 100–108.
[62] G. Moreno-Hagelsieb, B. Vitug, A. Medrano-Soto, M. H. Saier, *J. Mol. Microbiol. Biotechnol.* **2017**, *27*, 252–267.
[63] R. L. Fleischer, P. B. Price, R. M. Walker, *Nuclear Tracks in Solids: Principles and Applications*, University Of California Press, Oakland, **1975**.
[64] N. Fertig, C. Meyer, R. H. Blick, C. Trautmann, J. C. Behrends, *Phys. Rev. Stat. Nonlinear Soft Matter Phys.* **2001**, *64*, 409011–409014.
[65] A. J. Storm, J. H. Chen, X. S. Ling, H. W. Zandbergen, C. Dekker, *Nat. Mater.* **2003**, *2*, 537–540.
[66] J. Li, D. Stein, C. McMullan, D. Branton, M. J. Aziz, J. A. Golovchenko, *Nature* **2001**, *412*, 166–169.
[67] W. Li, N. A. W. Bell, S. Hernández-Ainsa, V. V. Thacker, A. M. Thackray, R. Bujdoso, U. F. Keyser, *ACS Nano* **2013**, *7*, 4129–4134.

[68] L. Luo, S. R. German, W. J. Lan, D. A. Holden, T. L. Mega, H. S. White, *Annu. Rev. Anal. Chem.* **2014**, *7*, 513–535.
[69] H. Kwok, K. Briggs, V. Tabard-Cossa, *PLoS One* **2014**, *9*, e92880.
[70] Y. M. N. D. Y. Bandara, B. I. Karawdeniya, J. R. Dwyer, *ACS Omega* **2019**, *4*, 226–230.
[71] C. Dekker, *Nat. Nanotechnol.* **2007**, *2*, 209–215.
[72] A. Siwy, Z. Fuliński, *Phys. Rev. Lett.* **2002**, *89*, 198103.
[73] K. Chuah, Y. Wu, S. R. C. Vivekchand, K. Gaus, P. J. Reece, A. P. Micolich, J. J. Gooding, *Nat. Commun.* **2019**, *10*, 2109.
[74] L. Xue, H. Yamazaki, R. Ren, M. Wanunu, A. P. Ivanov, J. B. Edel, *Nat. Rev. Mater.* **2020**, *5*, 931–951.
[75] L. Yang, J. Hu, M. C. Li, M. Xu, Z. Y. Gu, *Chem. Asian J.* **2022**, *17*, e202200775.
[76] Y. Goto, I. Yanagi, K. Matsui, T. Yokoi, K. I. Takeda, *Sci. Rep.* **2016**, *6*, 31324.
[77] R. H. Tunuguntla, R. Y. Henley, Y.-C. Yao, T. A. Pham, M. Wanunu, A. Noy, *Science* **2017**, *357*, 792–796.
[78] J. Feng, K. Liu, M. Graf, M. Lihter, R. D. Bulushev, D. Dumcenco, D. T. L. Alexander, D. Krasnozhon, T. Vuletic, A. Kis, A. Radenovic, *Nano Lett.* **2015**, *15*, 3431–3438.
[79] J. Feng, K. Liu, R. D. Bulushev, S. Khlybov, D. Dumcenco, A. Kis, A. Radenovic, *Nat. Nanotechnol.* **2015**, *10*, 1070–1076.
[80] P. W. K. Rothemund, *Nature* **2006**, *440*, 297–302.
[81] S. Dey, C. Fan, K. V. Gothelf, J. Li, C. Lin, L. Liu, N. Liu, M. A. D. Nijenhuis, B. Saccà, F. C. Simmel, H. Yan, P. Zhan, *Nat. Rev. Methods Primers* **2021**, *1*, 13.
[82] F. Hong, F. Zhang, Y. Liu, H. Yan, *Chem. Rev.* **2017**, *117*, 12584–12640.
[83] N. C. Seeman, H. F. Sleiman, *Nat. Rev. Mater.* **2017**, *3*, 17068.
[84] S. M. Douglas, H. Dietz, T. Liedl, B. Högberg, F. Graf, W. M. Shih, *Nature* **2009**, *459*, 414–418.
[85] H. Dietz, S. M. Douglas, W. M. Shih, *Science* **2009**, *325*, 725–730.
[86] Y. Ke, L. L. Ong, W. M. Shih, P. Yin, *Science* **2012**, *338*, 1177–1183.
[87] E. Benson, A. Mohammed, J. Gardell, S. Masich, E. Czeizler, P. Orponen, B. Högberg, *Nature* **2015**, *523*, 441–444.
[88] S. Nummelin, J. Kommeri, M. A. Kostiainen, V. Linko, *Adv. Mater.* **2018**, *30*, 1703721.
[89] Y. Hu, C. M. Niemeyer, *Adv. Mater.* **2019**, *31*, 1806294.
[90] N. C. Seeman, *Nature* **2003**, *421*, 427–431.
[91] S. Rinker, Y. Ke, Y. Liu, R. Chhabra, H. Yan, *Nat. Nanotechnol.* **2008**, *3*, 418–422.
[92] J. Sharma, R. Chhabra, A. Cheng, J. Brownell, Y. Liu, H. Yan, *Science* **2009**, *323*, 112–116.
[93] W. Liu, M. Tagawa, H. L. Xin, T. Wang, H. Emamy, H. Li, K. G. Yager, F. W. Starr, A. V. Tkachenko, O. Gang, *Science* **2016**, *351*, 582–586.
[94] A. Kuzyk, R. Schreiber, Z. Fan, G. Pardatscher, E. M. Roller, A. Högele, F. C. Simmel, A. O. Govorov, T. Liedl, *Nature* **2012**, *483*, 311–314.
[95] J. Fu, Y. R. Yang, A. Johnson-Buck, M. Liu, Y. Liu, N. G. Walter, N. W. Woodbury, H. Yan, *Nat. Nanotechnol.* **2014**, *9*, 531–536.
[96] J. J. Funke, H. Dietz, *Nat. Nanotechnol.* **2016**, *11*, 47–52.
[97] M. Madsen, K. V. Gothelf, *Chem. Rev.* **2019**, *119*, 6384–6458.
[98] Y. Yang, J. Wang, H. Shigematsu, W. Xu, W. M. Shih, J. E. Rothman, C. Lin, *Nat. Chem.* **2016**, *8*, 476–483.
[99] J. B. Knudsen, L. Liu, A. L. B. Kodal, M. Madsen, Q. Li, J. Song, J. B. Woehrstein, S. F. J. Wickham, M. T. Strauss, F. Schueder, J. Vinther, A. Krissanaprasit, D. Gudnason, A. A. A. Smith, R. Ogaki, A. N. Zelikin, F. Besenbacher, V. Birkedal, P. Yin, W. M. Shih, R. Jungmann, M. Dong, K. V. Gothelf, *Nat. Nanotechnol.* **2015**, *10*, 892–898.
[100] B. Shen, P. Piskunen, S. Nummelin, Q. Liu, M. A. Kostiainen, V. Linko, *ACS Appl. Bio Mater.* **2020**, *3*, 5606–5619.
[101] Y. L. Ying, J. Zhang, R. Gao, Y. T. Long, *Angew. Chem. Int. Ed.* **2013**, *52*, 13154–13161.
[102] L. Liu, H. C. Wu, *Angew. Chem. Int. Ed.* **2016**, *55*, 15216–15222.
[103] T. Ding, J. Yang, V. Pan, N. Zhao, Z. Lu, Y. Ke, C. Zhang, *Nucleic Acids Res.* **2020**, *48*, 2791–2806.
[104] Y. Xing, A. Dorey, L. Jayasinghe, S. Howorka, *Nat. Nanotechnol.* **2022**, *17*, 708–713.
[105] S. Howorka, S. Cheley, H. Bayley, *Nat. Biotechnol.* **2001**, *19*, 636–639.
[106] S. Howorka, L. Movileanu, O. Braha, H. Bayley, *Proc. Natl. Acad. Sci. USA* **2001**, *98*, 12996–13001.
[107] S. Howorka, H. Bayley, *Biophys. J.* **2002**, *83*, 3202–3210.
[108] W. Vercoutere, S. Winters-Hilt, H. Olsen, D. Deamer, D. Haussler, M. Akeson, *Nat. Biotechnol.* **2001**, *19*, 248–252.
[109] L. Franceschini, M. Soskine, A. Biesemans, G. Maglia, *Nat. Commun.* **2013**, *4*, 2415.
[110] J. Sánchez-Quesada, A. Saghatelian, S. Cheley, H. Bayley, M. R. Ghadiri, *Angew. Chem. Int. Ed.* **2004**, *43*, 3063–3067.
[111] Y. Wang, S. Zhang, W. Jia, P. Fan, L. Wang, X. Li, J. Chen, Z. Cao, X. Du, Y. Liu, K. Wang, C. Hu, J. Zhang, J. Hu, P. Zhang, H. Y. Chen, S. Huang, *Nat. Nanotechnol.* **2022**, *17*, 976–983.
[112] A. Henning-Knechtel, J. Knechtel, M. Magzoub, *Nucleic Acids Res.* **2017**, *45*, 12057–12068.
[113] E. Spruijt, S. E. Tusk, H. Bayley, *Nat. Nanotechnol.* **2018**, *13*, 739–745.
[114] A. Fennouri, J. List, J. Ducrey, J. Dupasquier, V. Sukyte, S. F. Mayer, R. D. Vargas, L. Pascual Fernandez, F. Bertani, S. Rodriguez Gonzalo, J. Yang, M. Mayer, *ACS Nano* **2021**, *15*, 11263–11275.
[115] T. Kurokawa, S. Kiyonaka, E. Nakata, M. Endo, S. Koyama, E. Mori, N. H. Tran, H. Dinh, Y. Suzuki, K. Hidaka, M. Kawata, C. Sato, H. Sugiyama, T. Morii, Y. Mori, *Angew. Chem. Int. Ed.* **2018**, *57*, 2586–2591.
[116] Q. Shen, Q. Xiong, K. Zhou, Q. Feng, L. Liu, T. Tian, C. Wu, Y. Xiong, T. J. Melia, C. P. Lusk, C. Lin, *J. Am. Chem. Soc.* **2023**, *145*, 1292–1300.
[117] Y. Jiang, A. Lee, J. Chen, V. Ruta, M. Cadene, B. T. Chait, R. MacKinnon, *Nature* **2003**, *423*, 33–41.
[118] C. C. Harrell, P. Kohli, Z. Siwy, C. R. Martin, *J. Am. Chem. Soc.* **2004**, *126*, 15646–15647.
[119] F. Xia, W. Guo, Y. Mao, X. Hou, J. Xue, H. Xia, L. Wang, Y. Song, H. Ji, Q. Ouyang, Y. Wang, L. Jiang, *J. Am. Chem. Soc.* **2008**, *130*, 8345–8350.
[120] X. Hou, W. Guo, F. Xia, F. Q. Nie, H. Dong, Y. Tian, L. Wen, L. Wang, L. Cao, Y. Yang, J. Xue, Y. Song, Y. Wang, D. Liu, L. Jiang, *J. Am. Chem. Soc.* **2009**, *131*, 7800–7805.
[121] Q. Kuang, P. Purhonen, H. Hebert, *Cell. Mol. Life Sci.* **2015**, *72*, 3677–3693.
[122] S. F. Buchsbaum, G. Nguyen, S. Howorka, Z. S. Siwy, *J. Am. Chem. Soc.* **2014**, *136*, 9902–9905.
[123] S. M. Iqbal, D. Akin, R. Bashir, *Nat. Nanotechnol.* **2007**, *2*, 243–248.
[124] A. Karmi, H. Dachlika, G. P. Sakala, D. Rotem, M. Reches, D. Porath, *ACS Appl. Nano Mater.* **2021**, *4*, 1000–1008.
[125] Y. Youn, C. Lee, J. H. Kim, Y. W. Chang, D. Y. Kim, K. H. Yoo, *Anal. Chem.* **2016**, *88*, 688–694.
[126] R. Ren, X. Wang, S. Cai, Y. Zhang, Y. Korchev, A. P. Ivanov, J. B. Edel, *Small Methods* **2020**, *4*, 2000356.
[127] A. R. Hall, A. Scott, D. Rotem, K. K. Mehta, H. Bayley, C. Dekker, *Nat. Nanotechnol.* **2010**, *5*, 874–877.
[128] G. C. Pugh, J. R. Burns, S. Howorka, *Nat. Chem. Rev.* **2018**, *2*, 113–130.
[129] N. A. W. Bell, C. R. Engst, M. Ablay, G. Divitini, C. Ducati, T. Liedl, U. F. Keyser, *Nano Lett.* **2012**, *12*, 512–517.

[130] R. Wei, T. G. Martin, U. Rant, H. Dietz, *Angew. Chem. Int. Ed.* **2012**, *51*, 4864–4867.
[131] P. Ketterer, A. N. Ananth, D. S. Laman Trip, A. Mishra, E. Bertosin, M. Ganji, J. Van Der Torre, P. Onck, H. Dietz, C. Dekker, *Nat. Commun.* **2018**, *9*, 902.
[132] S. Hernández-Ainsa, N. A. W. Bell, V. V. Thacker, K. Göpfrich, K. Misiunas, M. E. Fuentes-Perez, F. Moreno-Herrero, U. F. Keyser, *ACS Nano* **2013**, *7*, 6024–6030.
[133] C. Plesa, A. N. Ananth, V. Linko, C. Gü, A. J. Katan, H. Dietz, C. Dekker, *ACS Nano* **2014**, *8*, 35–43.
[134] S. Schmid, P. Stömmer, H. Dietz, C. Dekker, *Nat. Nanotechnol.* **2021**, *16*, 1244–1250.
[135] A. Barati Farimani, P. Dibaeinia, N. R. Aluru, *ACS Appl. Mater. Interfaces* **2017**, *9*, 92–100.
[136] C. Wen, E. Bertosin, X. Shi, C. Dekker, S. Schmid, *Nano Lett.* **2023**, *23*, 788–794.
[137] M. Langecker, V. Arnaut, T. G. Martin, J. List, S. Renner, M. Mayer, H. Dietz, F. C. Simmel, *Science* **2012**, *338*, 932–936.
[138] J. R. Burns, E. Stulz, S. Howorka, *Nano Lett.* **2013**, *13*, 2351–2356.
[139] J. R. Burns, K. Göpfrich, J. W. Wood, V. V. Thacker, E. Stulz, U. F. Keyser, S. Howorka, *Angew. Chem. Int. Ed.* **2013**, *52*, 12069–12072.
[140] J. R. Burns, N. Al-juffali, S. M. Janes, S. Howorka, *Angew. Chem. Int. Ed.* **2014**, *53*, 12466–12470.
[141] P. Chidchob, D. Offenbartl-Stiegert, D. McCarthy, X. Luo, J. Li, S. Howorka, H. F. Sleiman, *J. Am. Chem. Soc.* **2019**, *141*, 1100–1108.
[142] J. R. Burns, S. Howorka, *ACS Nano* **2018**, *12*, 3263–3271.
[143] O. Birkholz, J. R. Burns, C. P. Richter, O. E. Psathaki, S. Howorka, J. Piehler, *Nat. Commun.* **2018**, *9*, 1521.
[144] L. Messager, J. R. Burns, J. Kim, D. Cecchin, J. Hindley, A. L. B. Pyne, J. Gaitzsch, G. Battaglia, S. Howorka, *Angew. Chem. Int. Ed.* **2016**, *55*, 11106–11109.
[145] J. R. Burns, A. Seifert, N. Fertig, S. Howorka, *Nat. Nanotechnol.* **2016**, *11*, 152–156.
[146] A. Seifert, K. Göpfrich, J. R. Burns, N. Fertig, U. F. Keyser, S. Howorka, *ACS Nano* **2015**, *9*, 1117–1126.
[147] T. Diederichs, K. Ahmad, J. R. Burns, Q. H. Nguyen, Z. S. Siwy, M. Tornow, P. V. Coveney, R. Tampé, S. Howorka, *ACS Nano* **2021**, *15*, 16194–16206.
[148] P. M. Arnott, S. Howorka, *ACS Nano* **2019**, *13*, 3334–3340.
[149] C. Lanphere, P. M. Arnott, S. F. Jones, K. Korlova, S. Howorka, *Angew. Chem. Int. Ed.* **2021**, *60*, 1903–1908.
[150] D. Offenbartl-Stiegert, A. Rottensteiner, A. Dorey, S. Howorka, *Angew. Chem. Int. Ed.* **2022**, *61*, e202210886.
[151] R. Peng, L. Xu, H. Wang, Y. Lyu, D. Wang, C. Bi, C. Cui, C. Fan, Q. Liu, X. Zhang, W. Tan, *Nat. Commun.* **2020**, *11*, 978.
[152] C. Lv, X. Gu, H. Li, Y. Zhao, D. Yang, W. Yu, D. Han, J. Li, W. Tan, *ACS Nano* **2020**, *14*, 14616–14626.
[153] J. F. van Dyck, J. R. Burns, K. I. P. Le Huray, A. Konijnenberg, S. Howorka, F. Sobott, *Nat. Commun.* **2022**, *13*, 3610.
[154] K. Ahmad, A. Javed, C. Lanphere, P. V. Coveney, E. Orlova, S. Howorka, *Nat. Commun.* **2023**, https://doi.org/10.1038/s41467-023-38681-5.
[155] V. Maingi, J. R. Burns, J. J. Uusitalo, S. Howorka, S. J. Marrink, M. S. P. Sansom, *Nat. Commun.* **2017**, *8*, 14784.
[156] V. Maingi, M. Lelimousin, S. Howorka, M. S. P. Sansom, *ACS Nano* **2015**, *9*, 11209–11217.
[157] K. Göpfrich, T. Zettl, A. E. C. Meijering, S. Hernández-Ainsa, S. Kocabey, T. Liedl, U. F. Keyser, *Nano Lett.* **2015**, *15*, 3134–3138, 10.1038/s41467-023-38681-5.
[158] C. Lanphere, J. Ciccone, A. Dorey, N. Hagleitner-Ertuğrul, D. Knyazev, S. Haider, S. Howorka, *J. Am. Chem. Soc.* **2022**, *144*, 4333–4344.
[159] K. Göpfrich, C. Y. Li, I. Mames, S. P. Bhamidimarri, M. Ricci, J. Yoo, A. Mames, A. Ohmann, M. Winterhalter, E. Stulz, A. Aksimentiev, U. F. Keyser, *Nano Lett.* **2016**, *16*, 4665–4669.
[160] A. Ohmann, C. Y. Li, C. Maffeo, K. A. Nahas, K. N. Baumann, K. Göpfrich, J. Yoo, U. F. Keyser, A. Aksimentiev, *Nat. Commun.* **2016**, *9*, 2426.
[161] S. F. Jones, H. Joshi, S. J. Terry, J. R. Burns, A. Aksimentiev, U. S. Eggert, S. Howorka, *J. Am. Chem. Soc.* **2021**, *143*, 8305–8313.
[162] S. Krishnan, D. Ziegler, V. Arnaut, T. G. Martin, K. Kapsner, K. Henneberg, A. R. Bausch, H. Dietz, F. C. Simmel, *Nat. Commun.* **2016**, *7*, 12787.
[163] K. Göpfrich, C. Y. Li, M. Ricci, S. P. Bhamidimarri, J. Yoo, B. Gyenes, A. Ohmann, M. Winterhalter, A. Aksimentiev, U. F. Keyser, *ACS Nano* **2016**, *10*, 8207–8214.
[164] T. Diederichs, G. Pugh, A. Dorey, Y. Xing, J. R. Burns, Q. Hung Nguyen, M. Tornow, R. Tampé, S. Howorka, *Nat. Commun.* **2019**, *10*, 5018.
[165] R. P. Thomsen, M. G. Malle, A. H. Okholm, S. Krishnan, S. S. R. Bohr, R. S. Sørensen, O. Ries, S. Vogel, F. C. Simmel, N. S. Hatzakis, J. Kjems, *Nat. Commun.* **2019**, *10*, 5655.
[166] S. Dey, A. Dorey, L. Abraham, Y. Xing, I. Zhang, F. Zhang, S. Howorka, H. Yan, *Nat. Commun.* **2022**, *13*, 2271.
[167] Y. Li, C. Maffeo, H. Joshi, A. Aksimentiev, B. Ménard, R. Schulman, *Sci. Adv.* **2022**, *8*, eabq4834.
[168] A. M. Mohammed, R. Schulman, *Nano Lett.* **2013**, *13*, 4006–4013.
[169] Y. Li, R. Schulman, *Nano Lett.* **2019**, *19*, 3751–3760.
[170] A. M. Mohammed, P. Šulc, J. Zenk, R. Schulman, *Nat. Nanotechnol.* **2017**, *12*, 6703–6710.
[171] S. Yan, J. Zhang, Y. Wang, W. Guo, S. Zhang, Y. Liu, J. Cao, Y. Wang, L. Wang, F. Ma, P. Zhang, H.-Y. Chen, S. Huang, *Nano Lett.* **2021**, *21*, 6710.
[172] O. K. Zahid, B. S. Zhao, C. He, A. R. Hall, *Sci. Rep.* **2016**, *6*, 29565.
[173] E. Beamish, V. Tabard-Cossa, M. Godin, *ACS Sens.* **2019**, *4*, 2458–2464.
[174] J. Y. Y. Sze, A. P. Ivanov, A. E. G. Cass, J. B. Edel, *Nat. Commun.* **2017**, *8*, 1552.
[175] N. A. W. Bell, U. F. Keyser, *J. Am. Chem. Soc.* **2015**, *137*, 2035–2041.
[176] J. Kong, J. Zhu, K. Chen, U. F. Keyser, J. Kong, J. Zhu, K. Chen, U. F. Keyser, *Adv. Funct. Mater.* **2019**, *29*, 1807555.
[177] J. Kong, N. A. W. Bell, U. F. Keyser, *Nano Lett.* **2016**, *16*, 3557–3562.
[178] N. A. W. Bell, U. F. Keyser, *Nat. Nanotechnol.* **2016**, *11*, 645–651.
[179] J. Kong, J. Zhu, U. F. Keyser, *Chem. Commun.* **2017**, *53*, 436–439.
[180] F. Bošković, U. F. Keyser, *Nat. Chem.* **2022**, *14*, 1258–1264.
[181] S. Zhang, G. Huang, R. C. A. Versloot, B. M. H. Bruininks, P. C. T. de Souza, S. J. Marrink, G. Maglia, *Nat. Chem.* **2021**, *13*, 1192–1199.
[182] C. Lanphere, D. Offenbartl-Stiegert, A. Dorey, G. Pugh, E. Georgiou, Y. Xing, J. R. Burns, S. Howorka, *Nat. Protoc.* **2021**, *16*, 86–130.
[183] X. Shi, A. K. Pumm, J. Isensee, W. Zhao, D. Verschueren, A. Martin-Gonzalez, R. Golestanian, H. Dietz, C. Dekker, *Nat. Phys.* **2022**, *18*, 1105–1111.

Manuscript received: March 1, 2023
Accepted manuscript online: April 25, 2023
Version of record online: ■■, ■■

Aufsätze

DNA Nanotechnology

Y. Xing,* A. Rottensteiner, J. Ciccone, S. Howorka* —— **e202303103**

Functional Nanopores Enabled with DNA

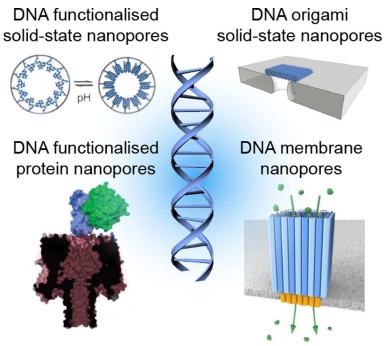

The scope of biological and synthetic nanopores can be structurally and functionally expanded by chemical modification with DNA as well as the creation of entirely DNA-based nanopores for applications in sensing, biological research, and synthetic biology.